

Spin relaxation and resonant phonon trapping in $[\text{Gd}_2(\text{fum})_3(\text{H}_2\text{O})_4]\cdot 3\text{H}_2\text{O}$

M. Orendáč, L. Sedláková, E. Čížmár, A. Orendáčová, and A. Feher

Centre of Low Temperature Physics, Faculty of Science, P. J. Šafárik University and Institute of Experimental Physics SAS, Park Angelinum 9, 041 54 Košice, Slovakia

S. A. Zvyagin and J. Wosnitza

Dresden High Magnetic Field Laboratory, FZ Dresden–Rossendorf, Germany

W. H. Zhu, Z. M. Wang, and S. Gao

Beijing National Laboratory for Molecular Sciences, State Key Laboratory of Rare Earth Materials Chemistry and Applications, College of Chemistry and Molecular Engineering, Peking University, 100871, China

(Received 10 November 2009; revised manuscript received 13 April 2010; published 9 June 2010)

Results of ac-susceptibility, specific-heat, magnetization, and electron-spin-resonance studies of a $[\text{Gd}_2(\text{fum})_3(\text{H}_2\text{O})_4]\cdot 3\text{H}_2\text{O}$ (fum=fumarate, $\text{C}_4\text{H}_2\text{O}_4$) powder samples are reported. The results of these measurements enabled us to identify the studied compound as a three-dimensional $S=7/2$ Heisenberg magnet with $T_N=0.19$ K and dominant crystal-field anisotropy. The susceptibility studies conducted at audio frequencies and temperatures from 2 to 30 K revealed that the application of static magnetic fields induces a slow spin relaxation. The relaxation is not associated with an anisotropy energy barrier and is explicable assuming resonant phonon trapping. The magnetic field dependence of the relaxation time is consistent with the proposed scenario and suggests that a strong spin-lattice interaction may be the mechanism governing the relaxation properties in the studied system.

DOI: [10.1103/PhysRevB.81.214410](https://doi.org/10.1103/PhysRevB.81.214410)

PACS number(s): 72.25.Rb, 74.25.Kc, 75.10.Dg, 75.40.Gb

I. INTRODUCTION

One of the key issues in magnetism and spintronics is to understand better the thermal relaxation of the magnetic system. This may either take place due to interactions between the spins or with other degrees of freedom, such as phonons or nuclear spins. Clarifying the mechanism of relaxation does not only represent a question of fundamental interest but also plays a key role in a possible tuning of the dynamic properties of magnetic materials with potential applications in magnetic cooling, data-storage techniques, or quantum computing.

Specifically, in single-molecule magnets, as potential representatives of qubits, the relaxation at low temperatures ($T < 1$ K) is usually governed by quantum tunneling,^{1,2} which can bring the spin system into thermal equilibrium with the lattice.³ In these materials as well as in diluted paramagnetic salts,^{4,5} the phonon-bottleneck (PB) effect has been found to influence the equilibration significantly. The PB effect sets in when the energy of the lattice modes created by the relaxing spins cannot be released into a thermal reservoir sufficiently fast. These lattice modes (“hot” phonons) may interact with the crystal boundaries only or may be reabsorbed by spins prolonging the equilibration time.

Indeed, the PB effect enabled the observation of a resonant quantum tunneling of the magnetization at 1.8 K in $(\text{Et}_4\text{N})_3\text{Fe}_2\text{Fe}_9$, (Ref. 6). Similarly, the formation of butterfly hysteresis loops in a V_{15} molecular complex⁷ and the relaxation behavior of the magnetization after a microwave pulse in single-molecule magnets containing Fe_8 (Ref. 8) or Cr_7Ni (Ref. 9) were attributed to a pronounced PB effect. Resonant trapping of low-energy phonons leading to the PB effect (Ref. 10) was proposed as a dominant mechanism responsible for the slow relaxation of the magnetization in Ni_{10}

magnetic molecules observed at higher temperatures (≈ 17 K).¹¹ Further, the PB effect, together with cross-spin relaxation, needed to be taken into account for a quantitative description of the temperature and magnetic field dependence of the relaxation time in the magnetically diluted $\text{LiYF}_4:\text{Ho}^{3+}$ system.¹²

On the other hand, the relaxation-time dependence on the crystal size, found, e.g., in $[\text{La}(\text{C}_2\text{H}_5\text{SO}_4)_3]\cdot 9\text{H}_2\text{O}$, magnetically diluted by Ce and Nd, (Ref. 13) and $\text{Cu}(\text{NH}_3)_2(\text{SO}_4)_2\cdot 6\text{H}_2\text{O}$, $\text{Gd}_2\text{Mg}_3(\text{NO}_3)_{12}\cdot 24\text{H}_2\text{O}$ (Ref. 14) below 4 K, suggested that scattering of phonons at crystal boundaries may be the limiting factor for the equilibration of the system.

A theoretical model for the PB effect based on first-principles calculations is still missing. Various simplified approaches have been adopted.¹⁵ In the present work, we address the relaxation properties of $[\text{Gd}_2(\text{fum})_3(\text{H}_2\text{O})_4]\cdot 3\text{H}_2\text{O}$, identified as a three-dimensional (3D) $S=7/2$ Heisenberg magnet with Neel ordering at $T_N=0.19$ K. It is suggested that the spin relaxation observed up to nominally 30 K, although much faster than reported in Refs. 6, 7, and 11, is governed predominantly by resonant phonon trapping in the studied system.

II. CRYSTAL STRUCTURE AND MAGNETIC INTERACTIONS

$[\text{Gd}_2(\text{fum})_3(\text{H}_2\text{O})_4]\cdot 3\text{H}_2\text{O}$ is isostructural to $[\text{Sm}_2(\text{fum})_3(\text{H}_2\text{O})_4]\cdot 3\text{H}_2\text{O}$, (Ref. 16). It crystallizes in the monoclinic space group $P21/n$ with unit-cell parameters $a=9.491(2)$ Å, $b=14.772(2)$ Å, $c=14.813(3)$ Å, $\beta=91.26(2)^\circ$, and $Z=4$. The structure is a 3D porous framework consisting of Gd-fum layers pillared by fum ligands,

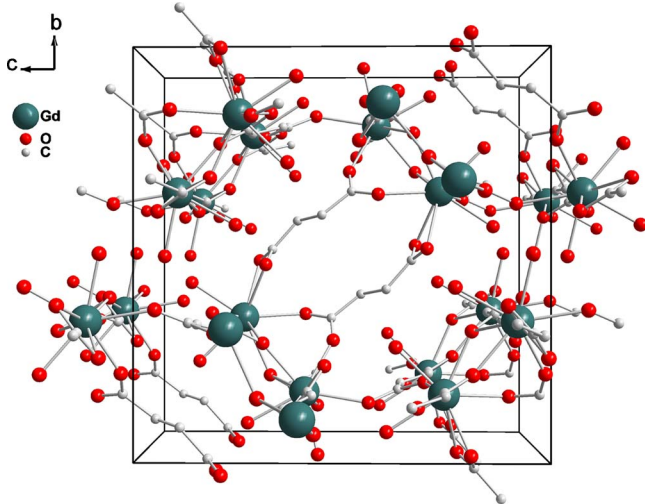


FIG. 1. (Color online) Schematic view of the crystal structure of $[\text{Gd}_2(\text{fum})_3(\text{H}_2\text{O})_4] \cdot 3\text{H}_2\text{O}$ viewed along the a axis. Hydrogen atoms and crystalline water are omitted for clarity.

with cavities occupied by hexameric water clusters. The basic structural unit is the Gd_2 dimer in which the two Gd^{3+} ions are bridged by two COO groups in chelating antimode from the two fum ligands, and further by a syn-syn COO group from the third fum ligand.

The Gd_2 dimers are interlinked into a wavy layer (Fig. 1) parallel to the ac plane through the first two fum ligands, then the layers are pillared by a third fum unit, to form the 3D framework. As adjacent wavy layers have troughs nearly opposite to each other, this framework of 3D pillared layers possesses cylindrical channels through the layers. However, the channels are divided into cavities by the fum pillars crossing the channels. Therefore, the framework is porous with cavities.

The Gd^{3+} ions have an environment of very distorted tri-capped trigonal prisms realized by the fum ligands and two coordinated water molecules. In addition, two magnetically nonequivalent Gd^{3+} positions are present in the structure. Since the Gd^{3+} ions are in the $S=7/2$ state with $L=0$, single-ion effects are negligible in first-order perturbation theory. However, strong spin-orbit coupling between the $4f$ electrons causes an admixture of $L \neq 0$ states to the Gd^{3+} ground state which leads to a single-ion anisotropy in second-order perturbation theory. Considering the large magnetic moment of the Gd^{3+} ions with $S=7/2$ as well as the distances between the Gd^{3+} ions in the lattice, varying from 4.14 to 9.48 Å, dipolar interactions may play a significant role in magnetic coupling. However, in the first approximation, the system can be described by a Hamiltonian involving a single-ion anisotropy D and an effective nearest-neighbor exchange coupling J , only,

$$\mathcal{H} = -J \sum_i S_i S_{i+1} + D \sum_i (S_i^z)^2 + g \mu_B B \sum_i S_i. \quad (1)$$

The third term in this expression represents the Zeeman energy, g stands for the g factor, and μ_B denotes the Bohr magneton.

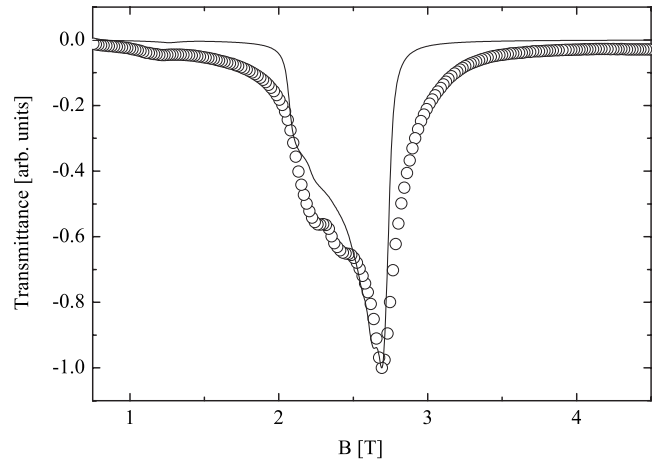


FIG. 2. Electron-spin-resonance line of $[\text{Gd}_2(\text{fum})_3(\text{H}_2\text{O})_4] \cdot 3\text{H}_2\text{O}$ obtained at 70 GHz and 1.75 K (circles). The solid line represents the result of the numerical simulation. See text for a more detailed discussion.

III. EXPERIMENTAL DETAILS

The specific heat of a powder sample, pressed into a pellet of 45 mg weight, was measured using a thermal-relaxation technique in a commercial dilution refrigerator. A RuO_2 thermometer (type RC 550), calibrated against a Lake Shore thermometer (LS 200A-50), was used to cover the temperature range from 150 mK to 3 K. The absolute accuracy of the specific heat is better than 5%. The powder sample was also used for electron-spin-resonance (ESR) measurements. The ESR experiments were performed in a tunable-frequency ESR spectrometer (similar to that described in Ref. 17) in the Faraday geometry at the Dresden High Magnetic Field Laboratory. The tunable-frequency ESR setup is composed of a 16 T high-homogeneity superconducting magnet and a set of tunable microwave sources. Phase-locked microwave sources from Virginia Diodes Inc. and a millimeter vector network analyzer (MVNA, product of AB Millimeter, Paris) were used. The microwave signals were detected by use of an InSb hot-electron bolometer (QMC Instruments Ltd.). The shape of the resonance line was analyzed using the “EASYSPIN” simulation package.¹⁸

The ac-susceptibility studies were performed using a commercial superconducting quantum interference device magnetometer (Quantum Design). For these measurements, 19.6 mg of the powder was placed in a gel cap which was held by a straw. The amplitude of the alternating magnetic field was 0.3 mT. The background contribution of the gel cap and straw is negligible below 30 K.

IV. RESULTS AND DISCUSSION

A. Estimation of single-ion anisotropy, exchange coupling, and dipolar interaction

The ESR spectrum was investigated at 1.75 K using a frequency of 70 GHz in magnetic fields up to 5 T and the data are shown in Fig. 2. The ESR line is characterized by a pronounced asymmetry with shoulders in the absorption at

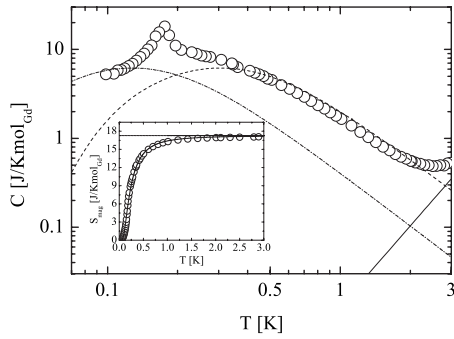


FIG. 3. Temperature dependence of the total specific heat of $[\text{Gd}_2(\text{fum})_3(\text{H}_2\text{O})_4]\cdot 3\text{H}_2\text{O}$ (circles). The lattice contribution is denoted by the solid line. The Schottky contributions to the specific heat calculated for an $S=7/2$ paramagnet with $D/k_B=-0.24$ K and $D/k_B=-0.1$ K are represented by dashed and dotted-dashed lines, respectively. Inset: temperature dependence of the magnetic entropy of $[\text{Gd}_2(\text{fum})_3(\text{H}_2\text{O})_4]\cdot 3\text{H}_2\text{O}$ (circles). The solid line represents a theoretical prediction for an $S=7/2$ paramagnet with $|D|/k_B=0.24$ K. The saturation value of the magnetic entropy for an $S=7/2$ paramagnet is denoted by the dashed line.

lower magnetic fields. Such a characteristic in the resonance line of Gd^{3+} clearly suggests an axial crystal-field anisotropy.¹⁹

The shape of the ESR line was analyzed to estimate the anisotropy introduced by crystal field. The analysis of the position and shape of the ESR line was performed using a single-ion approximation for $g=2.0$ and yields $D/k_B=-0.1$ K, $E/k_B=0.0035$ K, and $\Delta B=50$ mT, where E represents an in-plane anisotropy and ΔB denotes the width at half maximum. It should be stressed that including hyperfine interaction did not significantly alter the shape of the calculated resonance line. Therefore, nuclear degrees of freedom were not considered further. In spite of the oversimplified approach neglecting the two magnetically nonequivalent positions of the Gd^{3+} ions, the main features in the observed resonance line are reasonably well reproduced.

The specific heat was studied from 150 mK to 3 K in zero magnetic field. A dominant feature of the specific-heat data is a λ -like anomaly observed at 0.19 K indicating a phase transition (Fig. 3). Since the material studied is a magnetic insulator, only the magnetic and lattice subsystems contribute to the total specific heat. The lattice contribution was subtracted using the Debye approximation. More specifically, the lattice contribution was subtracted by finding the temperature region where the data may be described by the equation $C(T)=aT^{-2}+bT^3$. The bT^3 term represents the low-temperature lattice contribution in the Debye approximation while the aT^{-2} contribution describes the high-temperature behavior of the magnetic specific heat. For $1.3 \leq T \leq 3$ K, a least-squares fit yielded $a=(1.78 \pm 0.01)$ J K/mol and $b=(129.5 \pm 2.3) \times 10^{-4}$ J/(K⁴ mol). It should be noted that the value of the Debye temperature $\theta_D \approx 122$ K, resulting from the aforementioned analysis is rather small for the studied system and it might be associated with the low-energy vibrational modes arising from the presence of water molecules weakly bound in the porous structure. The resulting magnetic specific heat, C_{mag} , was used to calculate the mag-

netic entropy, which reaches the saturation value $R \ln(2S+1)$ expected for the $S=7/2$ system at about 2.5 K (inset of Fig. 3). This result supports the identification of the λ -like anomaly in specific heat as a manifestation of a magnetic ordering. In addition, the investigation of magnetocaloric effect in $[\text{Gd}_2(\text{fum})_3(\text{H}_2\text{O})_4]\cdot 3\text{H}_2\text{O}$ involving the critical region²⁰ revealed the existence of an inflection point in the isentropic line. This inflection point may be associated with the boundary between the ordered and disordered phase²¹ and for $[\text{Gd}_2(\text{fum})_3(\text{H}_2\text{O})_4]\cdot 3\text{H}_2\text{O}$ suggests shifting the critical temperature toward lower values with increasing magnetic field. Such a behavior is characteristic for systems with antiferromagnetic coupling. However, rather low temperature at which the saturation of the magnetic entropy occurs indicates the weakness of the antiferromagnetic correlations in the studied compound. Notably, the temperature dependence of the entropy, which was calculated from the specific-heat data, can be reproduced using the prediction for an $S=7/2$ paramagnet with a single-ion anisotropy of $|D|/k_B \approx 0.24$ K (solid line in the inset of Fig. 3) in a fair agreement with the estimation obtained from the analysis of ESR resonance line.

Further analysis of the magnetic entropy was performed by the comparison of the quantity $\Delta S_{\text{exp}}=(S_{\infty}-S_c)/R$, where S_{∞} denotes the saturation value of the entropy and S_c represents the value of the entropy at the critical temperature, calculated from the experimental data, with the corresponding quantity $\Delta S_{\text{theor}}^H$ predicted for a classical three-dimensional Heisenberg system with $z=6$.²² Since $S=7/2$ magnets can be considered as very good representatives of classical systems, striking disagreement between $\Delta S_{\text{theor}}^H=0.42$ and $\Delta S_{\text{exp}}=1.29$ reveals pronounced deviation of the magnetic behavior of $[\text{Gd}_2(\text{fum})_3(\text{H}_2\text{O})_4]\cdot 3\text{H}_2\text{O}$ from that anticipated in a three-dimensional Heisenberg magnet with only isotropic exchange interaction. On the other hand, easy-axis anisotropy deduced from the analysis of ESR resonance line may suggest that at low enough temperatures, only the lowest-energy levels will be occupied. If so, the system might be described by three-dimensional Ising model with the effective spin 1/2. Consequently, the quantity ΔS_{exp} may also be compared with $\Delta S_{\text{theor}}^I$ predicted for a three-dimensional Ising model with effective spin 1/2 and $z=6$, $\Delta S_{\text{theor}}^I=0.135$.²² The unsatisfactory agreement between $\Delta S_{\text{theor}}^I$ and ΔS_{exp} may be ascribed to the temperature dependence of the effective spin at low temperatures arising from a weak single-ion anisotropy.

Several approximations have been used to estimate the exchange coupling. More specifically, using a mean-field approach, the exchange interaction was obtained from the equation $k_B T_c/J=2/3zS(S+1)$, where T_c denotes the critical temperature and z stands for the number of the nearest neighbors. Taking $z=6$, the mean-field approximation yields $J/k_B=3$ mK while the method proposed by Rushbrooke and Wood²³ gives $J/k_B=4.1$ mK for $z=6$. The obtained magnitude of the exchange interaction suggests that $[\text{Gd}_2(\text{fum})_3(\text{H}_2\text{O})_4]\cdot 3\text{H}_2\text{O}$ belongs to the group of Heisenberg magnets with pronounced ($|D|>|J|$) single-ion anisotropy.²⁴⁻²⁶ However, the obtained values of exchange-coupling constant can be considered as a rough estimation only because in the aforementioned approaches, single-ion anisotropy was completely neglected. Generally, single-ion

anisotropy may have pronounced influence on the value of the ordering temperature.²⁷ On the other hand, the evaluation of the average dipolar coupling considering only two neighboring Gd^{3+} ions ($z=1$) results in $J_{dip}/k_B \approx 30$ mK.²⁸ This indicates that dipolar interactions play an important role in the magnetic ordering. More realistic estimation of the strength of dipolar coupling was obtained by calculating the dipolar field created by neighboring spins arranged in fully polarized state and antiferromagnetic configuration. In order to increase the accuracy of the estimation, the calculation involved 34 spins in a sphere of a radius 14 Å centered around the selected spin; the resulting dipolar energy $E_{dip}/k_B=0.29$ K for $S=7/2$ yields $J_{dip}/k_B \approx 24$ mK. The obtained result supports the role of dipolar interaction in the ordering process. It should be noted that dominant role of dipolar interaction was found in various classes of rare-earth-based magnetic insulators.^{29–31} The question arises whether more accurate estimation of D and J constants may be obtained using approaches successfully adopted in studying properties of model magnetic systems.^{22,32} However, to the best of our knowledge, the possibilities are limited. More specifically, standard spin-wave theory is inapplicable since for Heisenberg systems with arbitrary spin and $|D| > |J|$, apart from spin waves, single-ion bound states are formed in the same energy scale.³³ It may be anticipated that single-ion anisotropy will also influence thermodynamic properties above the critical temperature. This effect can be illustrated by comparing the experimental specific-heat data and Schottky contributions calculated for an $S=7/2$ paramagnet with $D/k_B=-0.24$ K and $D/k_B=-0.1$ K obtained from the analyses of the temperature dependence of the entropy and the shape of ESR resonance line, respectively, see Fig. 3. In addition, for the studied compound, the coupling within Gd_2 dimers present in the structure may also contribute to the observed high-temperature tail of the specific heat. Nevertheless, despite the differences in the values of the characteristic parameters D and J when using the different theoretical approaches, $[\text{Gd}_2(\text{fum})_3(\text{H}_2\text{O})_4] \cdot 3\text{H}_2\text{O}$ can be identified as an $S=7/2$ Heisenberg system with a strong ($|D| > |J|$) easy-axis anisotropy. Such an identification will enable the interpretation of the relaxation phenomena which are discussed below.

B. Determination of relaxation times

The ac susceptibility was studied from 2 to 30 K at various frequencies varying from 111 to 9999 Hz. Constant bias fields, B_{dc} , up to 3 T have been applied. Whereas the real parts of the susceptibility monotonically decrease with increasing temperature, the imaginary components form a broad maximum shifting toward higher temperatures with increasing modulation frequency (Fig. 4). However, out-of-phase signal was observed only for $B_{dc} \neq 0$.

Before discussing the temperature and magnetic field dependence of the relaxation time, the width of a potential distribution of the relaxation times should be addressed. The wide distribution of relaxation times may represent an intrinsic property of the studied system, e.g., spin glass, or might appear as a result of a powder nature of the sample. Cole-Cole formalism, based on the assumption of symmetric dis-

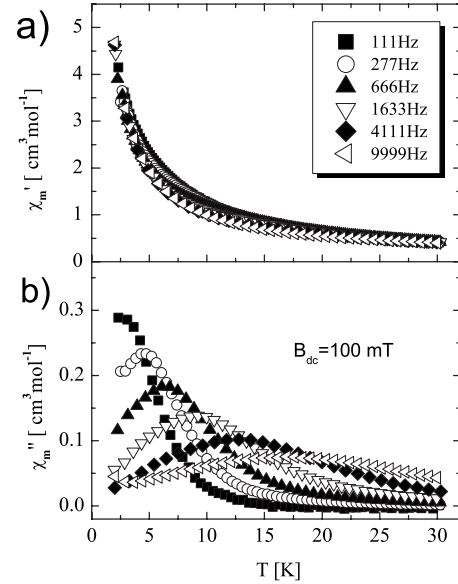


FIG. 4. Temperature dependence of the (a) real and (b) imaginary part of the ac susceptibility of $[\text{Gd}_2(\text{fum})_3(\text{H}_2\text{O})_4] \cdot 3\text{H}_2\text{O}$ in a magnetic field of 100 mT studied at frequencies from 111 to 9999 Hz.

tribution of the relaxation times in a logarithmic scale, was adopted for the analysis of ac-susceptibility data. Within this approach, the ac susceptibility may be described in the following form:

$$\chi(\omega) = \chi_{ad} + \frac{\chi_T - \chi_{ad}}{1 + (i\omega\tau_c)^{1-\alpha}}, \quad (2)$$

where χ_T and χ_{ad} represent isothermic and adiabatic susceptibilities, respectively, τ_c denotes a median relaxation time.³⁴ The parameter α determines the width of the distribution, $\alpha=0$ corresponds to the Debye relaxation with a single time constant whereas for $\alpha=1$, infinitely wide distribution may be anticipated. The values of the parameter α for $[\text{Gd}_2(\text{fum})_3(\text{H}_2\text{O})_4] \cdot 3\text{H}_2\text{O}$ were deduced from the analysis of Cole-Cole diagrams constructed for selected temperatures and magnetic fields, the results are presented in Fig. 5. The semicircle shape of the diagrams suggests a narrow distribution of the relaxation times. The parameter α was found to increase with decreasing temperature and to be only weakly dependent on magnetic field. In addition, the analysis reveals that $\alpha < 0.28$ for temperatures $5 < T < 20$ K and magnetic fields below 0.5 T. This value is much lower than that characterizing the relaxation in spin glasses.³⁵ It should be noted that $\alpha=0.456$ found in $\text{Dy}_2\text{Ti}_2\text{O}_7$ enabled describing the temperature dependence of the median relaxation time by standard Arrhenius formula assuming a single relaxation channel.³⁶ Notably, the pronounced decrease in χ_{ad}/χ_T was observed with increasing magnetic field. Such a decrease is consistent with the behavior found in $S=1/2$ paramagnet with a single relaxation time.³⁷ Consequently, in the subsequent analysis, the approach similar to that reported in Ref. 36 was used to study the behavior of τ_c in $[\text{Gd}_2(\text{fum})_3(\text{H}_2\text{O})_4] \cdot 3\text{H}_2\text{O}$.

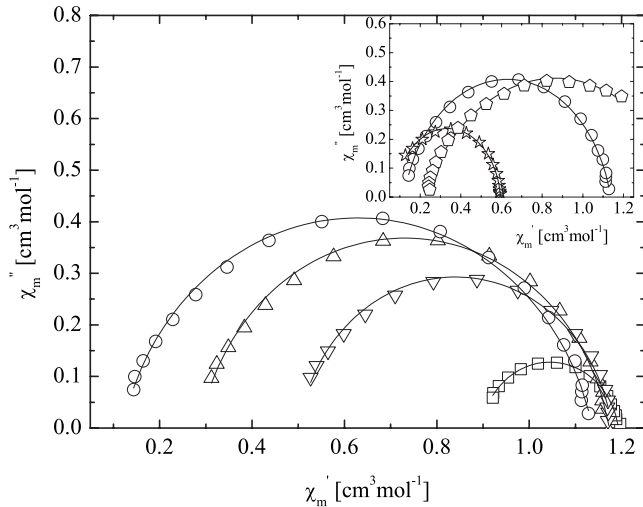


FIG. 5. Cole-Cole diagram studied at temperature 10 K for magnetic fields 0.1 T (squares, $\alpha=0.095$), 0.2 T (down triangles, $\alpha=0.093$), 0.3 T (up triangles, $\alpha=0.112$), and 0.5 T (circles, $\alpha=0.140$). Inset: Cole-Cole diagram studied at magnetic field 0.5 T and various temperatures 5 K (stars, $\alpha=0.279$), 10 K (circles, $\alpha=0.14$), and 20 K (pentagons, $\alpha=0.059$). The solid lines denote the results of fitting the data by the equation derived directly from Eq. (2), the resulting values of α for each temperature and magnetic field are given in parentheses. See text for a more detailed discussion.

More specifically, by using the positions of the broad maxima in the imaginary part of the susceptibility, the temperature and magnetic field dependence of τ_c , was extracted. This could be done with an accuracy of about 1.5%. The results are presented in Figs. 6 and 7. The ratio of the temperature at which the relaxation is observed and the value of the exchange coupling ($k_B T/J \approx 300$) makes the relaxation of collective degrees of freedom highly improbable.

Considering the values of the characteristic parameters and temperature, a single-ion approximation was adopted for the analysis of the obtained behavior of the median relaxation time. Here, the relaxation occurs through a transfer of the energy from the spins to the lattice modes, where the lattice is assumed to behave as a thermal reservoir. For single-spin relaxation, direct ($\tau^{-1} \approx T$), Raman ($\tau^{-1} \approx T^7$), and Orbach [$\tau^{-1} \approx \exp(\Delta/k_B T)$] relaxation processes are usually considered. However, as can be seen in the inset of Fig. 6, none of the aforementioned relaxation processes can describe the experimental data in the whole temperature range. Here, only the data measured at $B_{dc}=100$ mT are shown but similar results have been obtained for other fields. However, the data above 10 K might still suggest the presence of Orbach relaxation process. Indeed, fitting the data between 10 and 20 K assuming Orbach relaxation process leads to satisfactory agreement for $\Delta/k_B=36$ K. In contrast, this value clearly disagrees with the magnitude of the energy gap $|D|S^2/k_B=1.2$ K for $[\text{Gd}_2(\text{fum})_3(\text{H}_2\text{O})_4] \cdot 3\text{H}_2\text{O}$ with $D/k_B=-0.1$ K, obtained from the analysis of ESR data, excluding the possibility of Orbach relaxation process in the studied material.

The failure of the aforementioned approach suggests that the relaxation observed in $[\text{Gd}_2(\text{fum})_3(\text{H}_2\text{O})_4] \cdot 3\text{H}_2\text{O}$ cannot

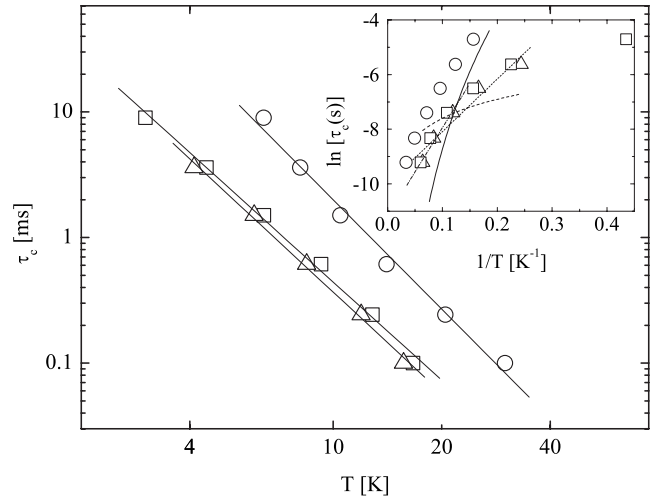


FIG. 6. Temperature dependence of the median relaxation time of $[\text{Gd}_2(\text{fum})_3(\text{H}_2\text{O})_4] \cdot 3\text{H}_2\text{O}$ studied at magnetic fields of 50 (triangles), 100 (squares), and 500 mT (circles). The solid lines represent corresponding fits using the relation $\tau = a * T^b$ yielding $b = -2.7 \pm 0.1$ for 50 mT, $b = -2.6 \pm 0.1$ for 100 mT, and $b = -2.9 \pm 0.1$ for 500 mT. Inset: temperature dependence of the median relaxation time in reduced coordinates. The data obtained at 100 mT were analyzed using the relations $\tau = a * T^{-1}$ (dashed line), $\tau = b * T^{-7}$ (solid line), and $\tau = c * \exp(-\Delta/k_B T)$ (short-dashed line). The dashed-dotted line denotes the result of fitting the data from 10 to 20 K using the relation $\tau = c * \exp(-\Delta/k_B T)$. See text for a more detailed discussion.

originate from the relaxation of a single spin to a phonon bath and the possibility of driving spins out of thermal equilibrium due to the PB effect could be taken into account. Generally, if the relaxation is governed by the PB effect, the temperature dependence of the relaxation time τ_{PB} for a two-level system can be approximated by $\tau^{-1} \approx T^2$ (Ref. 38). In order to explore whether such a situation occurs in the studied material at low magnetic fields, the temperature depen-

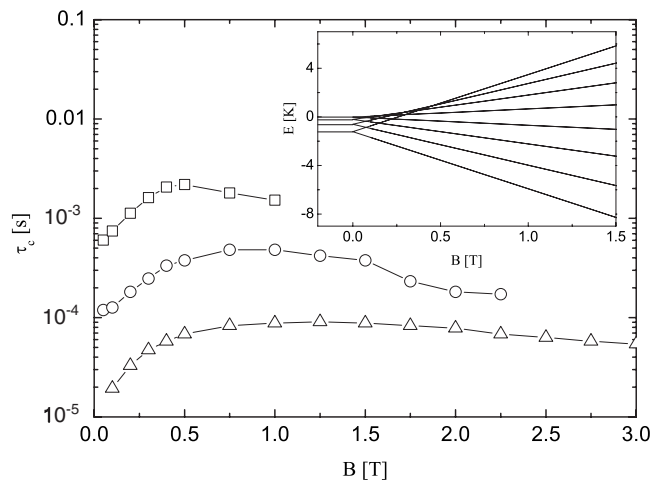


FIG. 7. Magnetic field dependence of the median relaxation time of $[\text{Gd}_2(\text{fum})_3(\text{H}_2\text{O})_4] \cdot 3\text{H}_2\text{O}$ studied at 5 (squares), 10 (circles), and 20 K (triangles). The solid lines are guide for the eyes. Inset: energy-level scheme for an $S=7/2$ paramagnet with $g=2.0$ and $D/k_B=-0.1$ K for $B \parallel z$.

dences of the median relaxation times obtained at 50, 100, and 500 mT were fitted using the formula $\tau_c = a * T^b$. The analysis resulted in $b = -2.7 \pm 0.1$ and $b = -2.6 \pm 0.1$ for the sets of data obtained at 50 mT and 100 mT, respectively, in reasonable agreement with the theoretical value of -2 .^{10,38} On the other hand, the value $b = -2.9 \pm 0.1$ extracted for the 500 mT data deviates more pronouncedly from the theoretical value. This presumably is an effect of the magnetic field. The fact that in the aforementioned range of temperatures and magnetic fields, the studied material does not represent a two-level system for which the discussed theoretical model was proposed, may represent another reason of the observed deviations. Indeed, for example, the temperature dependence of the relaxation time for Raman process in a multilevel spin system was found to be somewhat different from that in a two-level system.³⁹

The resonant phonon trapping may represent one of the mechanisms responsible for the onset of the PB effect.¹³ This trapping appears for a resonant phonon whose energy is nominally equal to the difference of the magnetic energy levels. Given that the wavelength of the resonant phonon exceeds the separation between magnetic ions, the phonon may repeatedly be absorbed and emitted. Consequently, coherent modes are formed and the energy is transferred to the lattice in much slower rate.¹⁰ It should be noted that the obtained temperature dependence of the median relaxation time supports the onset of the PB effect. However, the suggestion that the resonant phonon trapping is responsible for the observed behavior requires verification whether the conditions, under which the trapping may occur, are fulfilled. First of all, trapping of a resonant phonon in a magnetic system ultimately demands a sufficiently low exchange interaction. Indeed, if the interaction between the spins is strong, collective spin modes may transfer the energy of the excitation from the region where it was trapped originally. Nevertheless, as stated already, for the temperature range in which the slow relaxation was observed, the possibility of the formation of a collective spin excitation can be safely neglected. In addition, the resonant trapping requires wavelengths of the trapped phonons significantly larger than a typical distance between spin sites, namely, $k_0 r_{av} \ll 1$, where r_{av} is the average distance between magnetic Gd^{3+} ions and k_0 is the wave vector of the trapped phonon with the energy $h\nu_0$, in the first approximation equal to the difference between the energy levels of the magnetic ion. The latter can be calculated using the Debye approximation $h\nu_0 = v k_0$. The average sound velocity $v = 4.77 \times 10^3$ m/s can be estimated from the Debye temperature $\theta_D = 122$ K obtained from the specific-heat data.

The question arises which energy levels of the magnetic ion should be considered. Generally, if quantum tunneling is absent, the spin reversal from $S_z = 7/2$ to $S_z = -7/2$ and vice versa will be governed only by thermally activated process. Neglecting the selection rules for spin-phonon interaction,⁴⁰ all the excited states may be explored during the spin reversal.⁶ Although the selection rules may make some of the transitions “forbidden,” the excited states are involved during overcoming the energy barrier in a thermal-relaxation process which would be of Orbach type. Although, as mentioned above, this type of relaxation does not govern dy-

namic properties of the studied system, the excited states should be definitely involved in the analysis of the relaxation. This fact can be documented by the occupation of the energy levels at the temperatures where the anomalous relaxation was observed. For example, at $T = 5$ K and zero magnetic field, the calculation of the ratio of the occupation between the i th excited doublet and ground doublet given by the equation $n_i/n_0 = \exp(-\Delta E_i/k_B T)$, where ΔE_i denotes the energy difference between the ground state and the i th excited state, yields $n_1/n_0 = 0.89$, $n_2/n_0 = 0.82$, and $n_3/n_0 = 0.79$. The calculated ratios clearly suggest that considering only the transition between the ground state and the first excited state may not be adequate in full description of the observed relaxation process which may involve transitions between various energy levels.

Consequently, if the difference between the energy levels for $S_z = 1/2$ and $S_z = -1/2$ in a magnetic field of 50 mT is considered, the value $k_0 = 8.7 \times 10^6$ m⁻¹ is obtained. Taking into account $r_{av} = 6 \times 10^{-10}$ m leads to the resulting magnitude of $k_0 r_{av} \approx 10^{-3}$. Repeating the same calculation for the transitions from the state with $S_z = 7/2$ to $S_z = 5/2$ ($\Delta S_z = 1$) and also from the state $S_z = 7/2$ to $S_z = 3/2$ ($\Delta S_z = 2$) yields $k_0 r_{av} \approx 10^{-2}$ for both transitions. The obtained results support the efficiency of the resonant phonon trapping in $[Gd_2(fum)_3(H_2O)_4] \cdot 3H_2O$ in small magnetic fields for all possible transitions with $\Delta S_z = 1$ and $\Delta S_z = 2$.

Finally, the resonant phonon trapping may be suppressed by interactions between coherent modes and phonons from the thermal bath, where these phonons tend to destroy the coherence between the spins and, thus, isolate them from another. At temperatures at which such a process becomes significant, spin relaxation should occur at a time-scale characteristic for the energy transfer between one spin and a phonon from the bath.¹⁰ Consequently, a crossover in the temperature dependence of the relaxation time should appear when these decoherence effects become relevant. However, the density of the available experimental data does not enable the unambiguous determination of the crossover. Thus, the investigation of the potential crossover in the spin relaxation of $[Gd_2(fum)_3(H_2O)_4] \cdot 3H_2O$ represents the subject of subsequent studies.

C. Magnetic field dependence of the median relaxation time

The underlying mechanism of the spin relaxation may also be elucidated from the investigation of the magnetic field dependence of the median relaxation time. This study was performed in magnetic fields up to 3 T at selected temperatures 5, 10, and 20 K (Fig. 7). For all temperatures, the observed dependence is characterized by a broad maximum, the position of which is shifted upward with increasing temperature. In contrast, the magnitude of the maximum is inversely proportional to the temperature. The observed behavior does not seem to be in accord with the relaxation of a single spin to the phonon bath, where a monotonic magnetic field dependence of the relaxation is anticipated.³⁷ On the other hand, tentative explanation of the observed behavior may be based on considering the influence of the magnetic field on the resonant phonon trapping in the simplified model

describing the interaction of phonons with a two-level spin system. More specifically, for the two-level spin system, the probability of finding a state, where the trapped phonon is released and all spins are in the ground state, was theoretically studied in Ref. 10 and can be expressed as $P = \Delta\nu(k_0 r_{av})^3 / 4\pi\nu_0$, where $\Delta\nu$ denotes the bandwidth of phonons involved in the resonant trapping. It should be stressed that in the framework of the used theoretical model in a single-spin system, the probability P was found to be asymptotically equal to 1 prohibiting any resonant phonon trapping.¹⁰

The magnetic field dependence of the probability P can be qualitatively estimated by considering the relation $h\nu_0 = \nu k_0$ and taken into account the linear dependence of the energy separation $h\nu_0$ on magnetic field, yielding $P \approx B^2$. The obtained relation suggests that the growing energy-level difference in a magnetic field makes the spin relaxation more likely. Consequently, phonon trapping should be less effective and thus the relaxation time due to the PB effect should decrease with increasing magnetic field. This consideration is consistent with the experimental observation if the energy-level scheme of Gd^{3+} is taken into account. The simplified energy-level scheme is plotted in the inset of Fig. 6 considering only $D/k_B = -0.1$ K, $g = 2.0$, and $B \parallel z$, where several crossings of the energy levels occur in fields up to 0.4 T. A similar behavior is observed for other field orientations, only the crossings are shifted toward higher fields.

The energy-level scheme reveals that below 0.4 T for selected transitions (e.g., $7/2 \rightarrow 5/2$, $5/2 \rightarrow 3/2$, and $3/2 \rightarrow 1/2$), an increasing magnetic field *decreases* the difference between the energy levels, making resonant phonon trapping for these levels more efficient. On the other hand, the opposite behavior may be anticipated for magnetic fields higher than ~ 0.4 T where an increasing magnetic field increases the separation between all energy levels. As a result, a broad maximum in the magnetic field dependence of the τ_c due to the PB effect may be expected for the studied material in accord with the experimental observation.

The shift of the median relaxation time to lower values observed for higher temperatures might also be attributed to phonons from the thermal bath interacting with the trapped ones introducing an additional relaxation channel and thus making the relaxation more probable.

V. CONCLUSION

In conclusion, the analysis of the specific heat, magnetic entropy, and shape of the ESR line enabled the identification of $[\text{Gd}_2(\text{fum})_3(\text{H}_2\text{O})_4] \cdot 3\text{H}_2\text{O}$ as an $S = 7/2$ magnetic Heisenberg system with pronounced easy-axis anisotropy. The investigation of the ac susceptibility in different bias fields revealed the onset of a slow spin relaxation. The temperature dependence of the median relaxation time supports resonant phonon trapping leading to the phonon-bottleneck effect as the relevant mechanism governing the relaxation. This suggestion is consistent with the simplified analysis of the magnetic field dependence of the median relaxation time using a single-ion approximation. Consequently, apart from magnetically diluted salts and single-molecule magnets, $[\text{Gd}_2(\text{fum})_3(\text{H}_2\text{O})_4] \cdot 3\text{H}_2\text{O}$ seems to represent another system in which resonant phonon trapping plays a crucial role.

It may be interesting to investigate the effect of resonant phonon trapping in transport properties since the trapped phonons may contribute to a decreasing thermal conductivity, the decrease being controlled by magnetic field. In addition, a more detailed quantitative analysis will be required to incorporate hyperfine interactions as well as synthesis of an $S = 1/2$ compound with structure and magnetic properties similar to $[\text{Gd}_2(\text{fum})_3(\text{H}_2\text{O})_4] \cdot 3\text{H}_2\text{O}$. Nevertheless, for these steps, single crystals of sufficient size would be needed for corresponding experimental studies. An ongoing effort is devoted to their synthesis.

ACKNOWLEDGMENTS

The work was supported by several grants. More specifically, experimental studies of specific heat, electron-spin resonance, and ac susceptibility were supported by projects APVV LPP-0102-06, EuroMagNet (EU Contract No. 228043) and 973-2006CB601102, respectively. L. S. gratefully acknowledges support of APVV LPP-0102-06 in her Ph.D. studies. A. O., M. O., and E. C. acknowledge the kind hospitality of Peking University during their stay, which was supported by SK-CN-0032-07 and enabled common work on the manuscript. In addition, projects VEGA 1/0078/09 partially supported the visit of E. C. to the Dresden High Magnetic Field Laboratory. Material support of U. S. Steel is also gratefully acknowledged.

¹W. Wernsdorfer, T. C. Stamatatos, and G. Christou, *Phys. Rev. Lett.* **101**, 237204 (2008).

²A. Morello and L. J. de Jongh, *Phys. Rev. B* **76**, 184425 (2007).

³M. Evangelisti, F. Luis, F. L. Mettes, N. Aliaga, G. Aromi, J. J. Alonso, G. Christou, and L. J. de Jongh, *Phys. Rev. Lett.* **93**, 117202 (2004).

⁴F. R. Nash, *Phys. Rev.* **138**, A1500 (1965).

⁵J. Wooldridge, *Phys. Rev.* **185**, 602 (1969).

⁶R. Schenker, M. N. Leuenberger, G. Chaboussant, D. Loss, and H. U. Gudel, *Phys. Rev. B* **72**, 184403 (2005).

⁷I. Chiorescu, W. Wernsdorfer, A. Müller, H. Bögge, and B. Bar-

bara, *Phys. Rev. Lett.* **84**, 3454 (2000).

⁸K. Petukhov, S. Bahr, W. Wernsdorfer, A. L. Barra, and V. Mosser, *Phys. Rev. B* **75**, 064408 (2007).

⁹W. Wernsdorfer, D. Mailly, G. A. Timco, and R. E. P. Winpenny, *Phys. Rev. B* **72**, 060409(R) (2005).

¹⁰D. L. Huber, *Phys. Rev.* **139**, A1684 (1965).

¹¹S. Carretta, P. Santini, G. Amoretti, M. Affronte, A. Candini, A. Ghirri, I. S. Tidmarsh, R. H. Laye, R. Shaw, and E. J. L. McInnes, *Phys. Rev. Lett.* **97**, 207201 (2006).

¹²S. Bertaina, B. Barbara, R. Giraud, B. Z. Malkin, M. V. Vanuy- nin, A. I. Pominov, A. L. Stolov, and A. M. Tkachuk, *Phys. Rev.*

- B **74**, 184421 (2006).
- ¹³P. L. Scott and C. D. Jeffries, *Phys. Rev.* **127**, 32 (1962).
- ¹⁴J. A. Giordmaine, L. E. Alsop, F. R. Nash, and C. H. Townes, *Phys. Rev.* **109**, 302 (1958).
- ¹⁵D. A. Garanin, *Phys. Rev. B* **77**, 024429 (2008), and references therein.
- ¹⁶S. C. Manna, E. Zangrando, J. Ribas, and N. R. Chaudhuri, *Polyhedron* **25**, 1779 (2006).
- ¹⁷S. A. Zvyagin, J. Krzystek, P. H. M. van Loosdrecht, G. Dhalenne, and A. Revcolevschi, *Physica B* **346-347**, 1 (2004).
- ¹⁸S. Stoll and A. Schweiger, *J. Magn. Reson.* **178**, 42 (2006).
- ¹⁹J. N. Glazkov, A. I. Smirnov, J. P. Sanchez, A. Forget, D. Colson, and P. Bonville, *J. Phys.: Condens. Matter* **18**, 2285 (2006).
- ²⁰L. Sedláková, J. Hanko, A. Orendáčová, M. Orendáč, C. L. Zhou, W. H. Zhu, B. W. Wang, Z. M. Wang, and S. Gao, *J. Alloys Compd.* **487**, 425 (2009).
- ²¹J. H. Schelleng and S. A. Friedberg, *Phys. Rev.* **185**, 728 (1969).
- ²²L. J. De Jongh and A. R. Miedema, *Adv. Phys.* **50**, 947 (2001).
- ²³G. S. Rushbrooke and P. J. Wood, *Mol. Phys.* **1**, 257 (1958).
- ²⁴S. Cox, R. D. McDonald, M. Armanious, P. Sengupta, and A. Paduan-Filho, *Phys. Rev. Lett.* **101**, 087602 (2008).
- ²⁵N. Papanicolaou and P. N. Spathis, *Phys. Rev. B* **52**, 16001 (1995).
- ²⁶D. L. Meier, M. Karnezos, and S. A. Friedberg, *Phys. Rev. B* **28**, 2668 (1983).
- ²⁷J. Strečka, J. Dely, and L. Čanová, *Chin. J. Phys.* **46**, 329 (2008).
- ²⁸C. M. Wynn, M. A. Girtu, W. B. Brinckerhoff, K. I. Sugiura, J. S. Miller, and A. J. Epstein, *Chem. Mater.* **9**, 2156 (1997).
- ²⁹J. M. Daniels, M. T. Hirvonen, A. P. Jauho, T. E. Katila, and K. J. Riski, *Phys. Rev. B* **11**, 4409 (1975).
- ³⁰A. Orendáčová, D. Horváth, M. Orendáč, E. Čižmár, M. Kačmár, V. Bondarenko, A. G. Anders, and A. Feher, *Phys. Rev. B* **65**, 014420 (2001).
- ³¹J. Snyder, J. S. Slusky, R. J. Cava, and P. Schiffer, *Nature (London)* **413**, 48 (2001).
- ³²R. L. Carlin and F. Palacio, *Coord. Chem. Rev.* **65**, 141 (1985).
- ³³R. Silbergliitt and J. B. Torrance, Jr., *Phys. Rev. B* **2**, 772 (1970).
- ³⁴C. Dekker, A. F. M. Arts, H. W. de Wijn, A. J. van Duynveldt, and J. A. Mydosh, *Phys. Rev. B* **40**, 11243 (1989).
- ³⁵J. A. Mydosh, *Spin Glasses: An Experimental Introduction* (Taylor & Francis, Washington, DC, 1993).
- ³⁶K. Matsuhira, Y. Hinatsu, and T. Sakakibara, *J. Phys.: Condens. Matter* **13**, L737 (2001).
- ³⁷R. L. Carlin and A. J. van Duynveldt, *Magnetic Properties of Transition Metal Compounds* (Springer-Verlag, New York, 1977).
- ³⁸A. C. Anderson and J. E. Robichaux, *Phys. Rev. B* **3**, 1410 (1971).
- ³⁹R. Orbach and M. Blume, *Phys. Rev. Lett.* **8**, 478 (1962).
- ⁴⁰R. D. Mattuck and M. W. P. Strandberg, *Phys. Rev.* **119**, 1204 (1960).